Dynamic Properties of Aircraft Tires

S. K. Clark,* R. N. Dodge,† and G. H. Nybakken‡
University of Michigan, Ann Arbor, Mich.

A research program has investigated the use of the von Schlippe string-type tire model for predicting the dynamic behavior of aircraft tires. The transfer function method was used for theory evaluation. A more flexible two constant modification to the string theory tire model is presented. Experiments were conducted on four types of scale model aircraft tires. Two types were of conventional bias construction, one type was an isotropic toroid and one type was of unbelted radial construction. The conventional string theory model gave predictions that were in good agreement with experimental data for bias constructed tires. The two constant modification to string theory provided better agreement beween predictions and experiment for the unconventional tires. The results indicate that the string theory tire model using static and slow-rolling tire properties predicts dynamic aircraft tire properties that have the same trends as the measured dynamic properties and, in most cases, provides good quantitative agreement.

Nomenclature

C_F = dynamic lateral force coefficient
C_M = dynamic moment coefficient
D = tire diameter
F_y = side force normal to wheel plane
F_z = vertical force
h = tire footprint half length
$k_{F\phi}$ = tire force yaw stiffness
k_{Mz} = tire moment yaw stiffness
k_y = tire lateral stiffness
M_z = moment about vertical axis
p_o = tire inflation pressure
s = tire path distance
t = time
v_o = road speed
x = distance from reference line to wheel plane center
x_o = lateral displacement excitation amplitude
y = distance from reference line to front of tire contact line
$\bar{y}$ = distance from reference line to rear of tire contact line
z = distance from wheel plane to front of tire contact line
$\bar{z}$ = distance from wheel plane to rear of tire contact line
α = phase angle defined by Eq. (14)
λ = tire relaxation length
ϕ = yaw angle between reference line and wheel plane
ϕ_0 = steer excitation amplitude
Ω = input excitation frequency

Introduction

THE problem of shimmy of rolling wheels on taxiing aircraft has been of interest for many years. Theoretical tire models used to investigate shimmy can, in general, be divided into two groups. Both tire models result in a tire force output given by a first order differential equation. Von Schlippe[1] proposed a tire model based on a stretched string supported by an elastic foundation, which includes a path delay constant called the relaxation length. Moreland[2] proposed a more empirical tire model which uses a time delay constant. Unfortunately, there is no obvious way to relate these two tire models. The purpose of this investigation is to assess the von Schlippe string tire model using measurements of dynamic tire properties.

A previous paper[3] showed that scale model aircraft tires could be constructed to represent most of the mechanical properties of full size aircraft tires. Two tires of conventional bias construction as well as two tires of less conventional construction are used in this study to determine the adequacy of string theory as a basis for a mathematical model for dynamic tire behavior in general and tire shimmy predictions in particular.

Tire Model Using the String on Elastic Foundation

One accepted method of comparing theoretical predictions with experimental results in dynamics involves the use of a transfer function. Forced coordinate excitation is applied to the system and the resulting forces and moments are measured. The resulting transfer function can be compared to the theoretical predictions for evaluation of the particular theoretical model. This procedure is used in the present study. String theory predictions will be developed for forced motion input.

The tire model of von Schlippe[1] is based on two assumptions. The first is that the tire force output is proportional to some characteristic deflection of the contact patch relative to the wheel plane. Referring to Fig. 1, the specific relation assumes the contact line is straight between the leading edge of the contact length (with deflec-

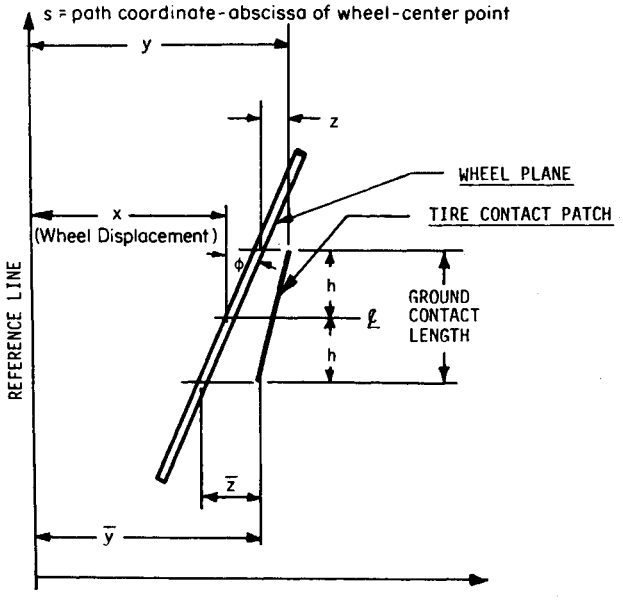

Fig. 1 Geometry for tire contact analysis.

Received August 3, 1973. This work was supported by NASA Langley Research Center, under Grant NGL 23-005-010.
Index category: Aircraft Landing Dynamics.
*Professor of Applied Mechanics and Engineering Science.
†Research Assistant, Applied Mechanics.
‡Research Associate, Applied Mechanics.

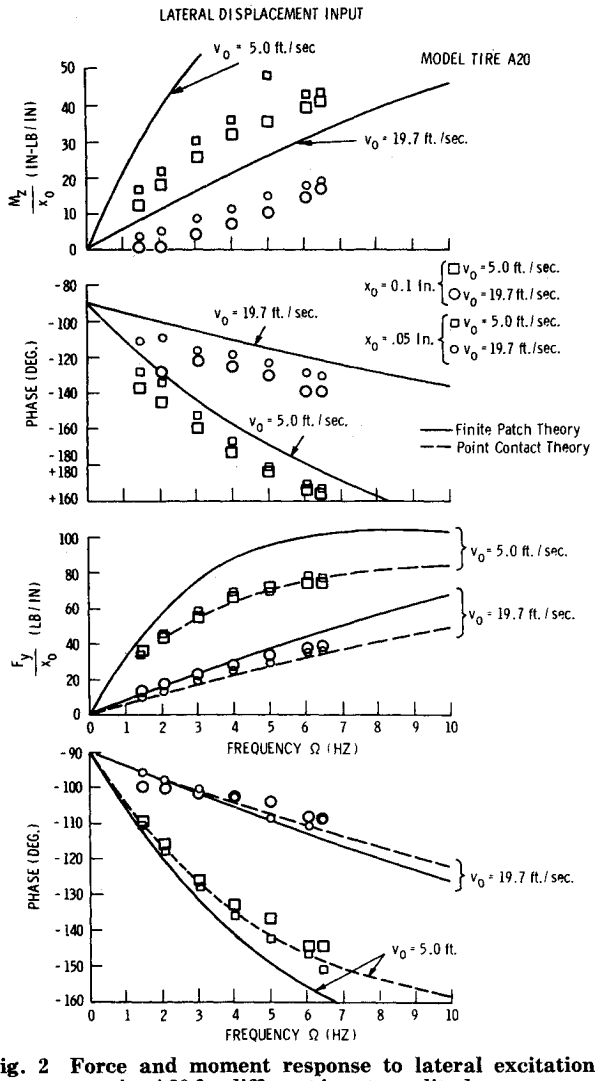

Fig. 2 Force and moment response to lateral excitation of tire A20 for different input amplitudes.

tion z) and the trailing edge of the contact length (with deflection $\bar{z}$). The resulting force is given by

$$F_y = k_y(\bar{z} + z)/2 \tag{1}$$

where F_y is the lateral force output of the tire and k_y is the tire static lateral stiffness. The second assumption is based on an exponential decay curve for the centerline deflection outside the contact patch, in the form

$$(dz/ds) = -(z/\lambda) \tag{2}$$

where λ is the relaxation length. This is identical to the form taken by a string under tension when supported by an elastic foundation. Using the geometry in Fig. 1 and assuming small angles, the tracking Eq. (2) becomes

$$(dy/ds) + (1/\lambda)\, y = (1/\lambda)\, x + \phi\, [(1 + (1/\lambda)\, h] \tag{3}$$

where x and ϕ define the wheel plane, h is the half length of the contact line and y defines the front of the contact line relative to the reference line. Geometry also requires that

$$z = y - x - h\phi \tag{4}$$

and

$$\bar{z} = \bar{y} - x + h\phi \tag{5}$$

A point contact theory can be developed by letting h go to zero in Eqs. (3-5). For a finite contact length, the rear deflection is defined by introducing a delay length of $2h$ into the expression for the front deflection

$$\bar{y}(s) = y(s - 2h) \tag{6}$$

Since z and $\bar{z}$ are, in general, not equal, a self-aligning torque is also predicted

$$M_z = k_y\left(\frac{\bar{z} - z}{2}\right)\left[\lambda + \frac{h^2}{3(\lambda + h)}\right] \tag{7}$$

The relations Eqs. (3) and (6) can be transformed to the time domain by using $s = v_0 t$, where v_0 is the road speed and is considered constant.

The two coordinates defining the wheel plane, x and ϕ, suggest two modes of forced input, lateral, and steer excitation. Using either

$$\phi = \phi_o \sin \Omega t \tag{8}$$

or

$$x = x_o \sin \Omega t \tag{9}$$

as input excitation, expressions for the force and moment response using Eqs. (1-7) can be derived.

The resulting expressions for lateral excitation, $x = x_0 \sin\Omega t$, are

$$\text{force amplitude} = 1/2\; k_y x_o \left|\cos\alpha\right| \left[\left(1 - \cos\frac{2h\Omega}{v_o}\right)^2 + \left(\sin\frac{2h\Omega}{v_o} + 2\,\frac{\lambda\Omega}{v_o}\right)^2\right]^{1/2} \tag{10}$$

$$\text{force phase} = \arctan\left(\frac{-\sin\frac{2h\Omega}{v_o} - 2\,\frac{\lambda\Omega}{v_o}}{\cos\frac{2h\Omega}{v_o} - 1}\right) + \alpha \tag{11}$$

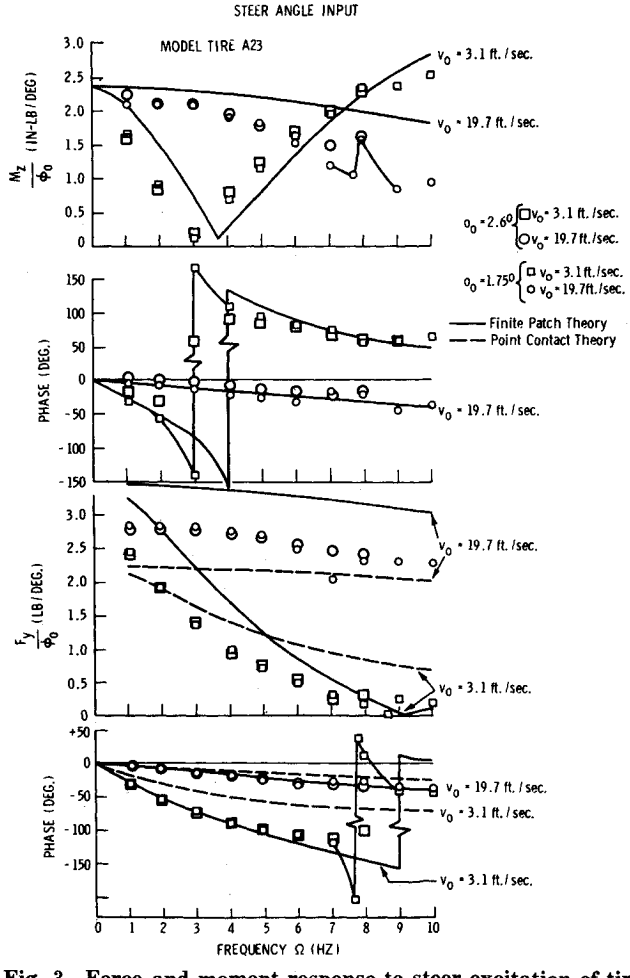

Fig. 3 Force and moment response to steer excitation of tire A23 for different input amplitudes.

Table 1 Tire operating conditions and static tire elastic properties

Tire	Type	p_0 psi	D in.	F_z lb	(h/D)	(λ/D)	k_y lb/in.
A20	2-ply bias-scaled 40 × 12-14 PR Type VII	25	4.53	50	0.202	0.523	91
A23	2-ply bias-scaled 40 × 12-14 PR Type VII	19.5	4.61	41	0.214	0.390	71
A24	2-ply bias-scaled 40 × 12-14 PR Type VII	21	4.58	44	0.214	0.304	76
B9	2-ply bias-scaled 49 × 17-26 PR Type VII	25	4.08	41	0.202	0.363	84
VecoCL	Isotropic toroid	5	4.54	11	0.182	0.355	18
RHCA12	1-ply unbelted radial	10	4.68	23	0.214	0.327	24

and

torque amplitude

$$= k_y\left[\lambda + \frac{h^2}{3(\lambda + h)}\right] x_o \left| \cos\alpha \sin\frac{h\Omega}{v_o} \right| \quad (12)$$

$$\text{torque phase} = \arctan\left(\frac{-\sin\dfrac{2h\Omega}{v_o}}{\cos\dfrac{2h\Omega}{v_o} - 1}\right) + \alpha \quad (13)$$

where α is defined by

$$\tan\alpha = -\lambda\Omega/v_o \quad (14)$$

The appropriate expressions for the point contact theory can be derived from Eqs. (10–14) by letting $h \to 0$. For the point contact theory the torque magnitude is zero, which might be expected since $z = \bar{z}$.

For steer excitation, $\phi = \phi_0 \sin\Omega t$, the resulting expressions are

$$\text{force amplitude} = k_y(h + \lambda)\phi_o \left| \cos\alpha \cos\frac{h\Omega}{v_o} \right| \quad (15)$$

$$\text{force phase} = \arctan\left(\frac{-\sin\dfrac{2h\Omega}{v_o}}{\cos\dfrac{2h\Omega}{v_o} + 1}\right) + \alpha \quad (16)$$

and

$$\text{torque amplitude} = 1/2\, k_y\left[\lambda + \frac{h^2}{3(\lambda + h)}\right] \phi_o$$

$$\left\{\left[(\lambda - h)\cos\alpha - (\lambda + h)\cos\alpha \cos\frac{2h\Omega}{v_o}\right]^2\right.$$

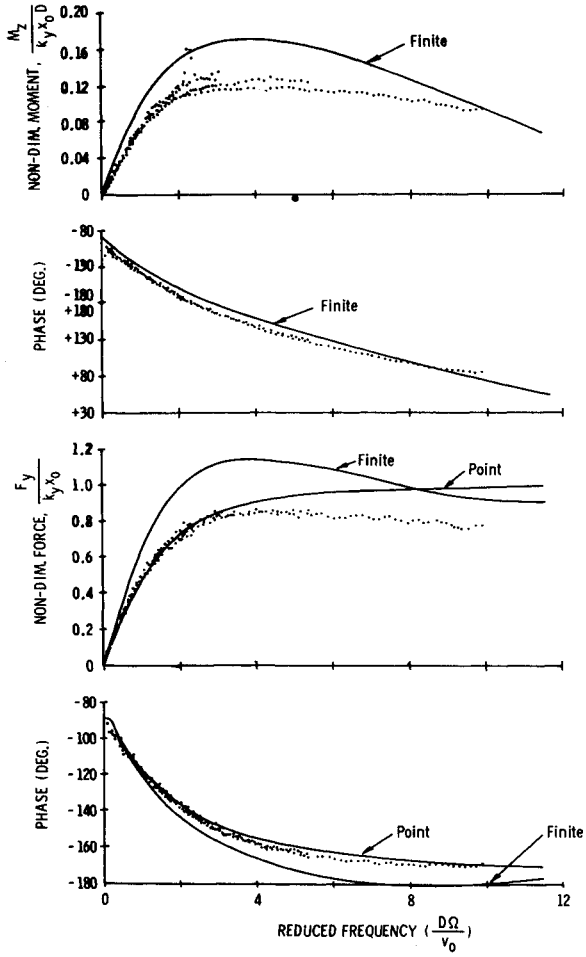

Fig. 4 Dimensionless force and moment response to lateral excitation of tire A20.

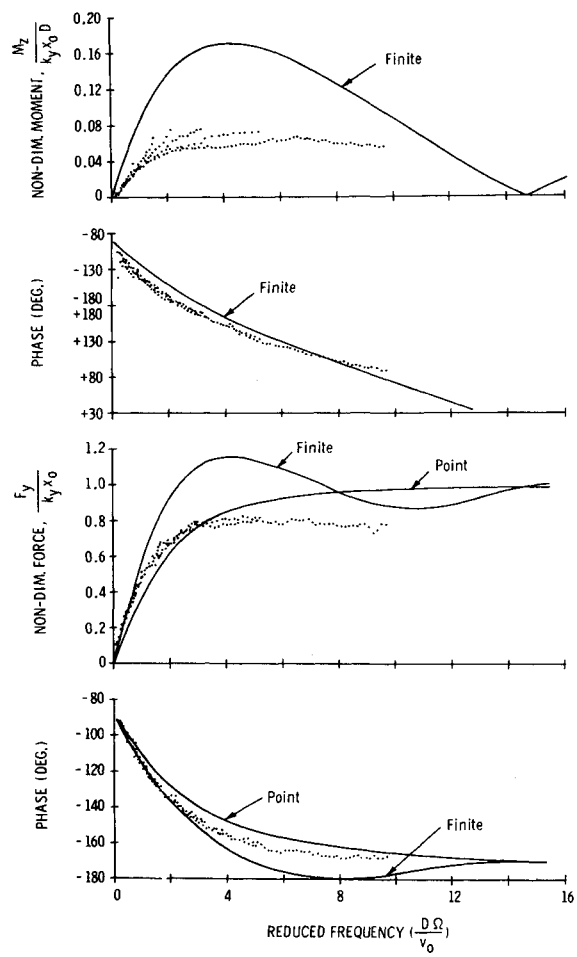

Fig. 5 Dimensionless force and moment response to lateral excitation of tire A23.

$$+\left[(\lambda + h)\cos\alpha\sin\frac{2h\Omega}{v_o} - 2h\sin\alpha\right]^2\Bigg\}^{1/2} \quad (17)$$

$$\text{torque phase} = \arctan\left(\frac{2\dfrac{\lambda h\Omega}{v_o} - (\lambda + h)\sin\dfrac{2h\Omega}{v_o}}{(\lambda + h)\cos\dfrac{2h\Omega}{v_o} - (\lambda - h)}\right) + \alpha \quad (18)$$

where α is given by Eq. (14). Again the point contact predictions are derived from Eqs. (15-18) by letting $h \to 0$. Again no torque is predicted by point contact theory.

A modification to the expressions for the force and moment output of the tire, Eqs. (1) and (7), respectively, can be accomplished by using the more general expressions

$$F_y = C_F\left(\frac{\bar{z} + z}{2}\right) \quad (19)$$

and

$$M_z = C_M\left(\frac{\bar{z} - z}{2}\right) \quad (20)$$

C_F and C_M are, respectively, a dynamic lateral force coefficient and a dynamic self-aligning torque coefficient. These coefficients can be related directly to the tire cornering power. For small steady-state yaw angles, there is a linear relationship between the steer angle and the resulting force and moment,

$$\left.\begin{aligned} F_y &= k_{F\phi}\,\phi \\ \text{and} \\ M_z &= k_{Mz}\phi \end{aligned}\right\} \quad (21)$$

String theory relates the yaw force spring constant $k_{F\phi}$ and the lateral force coefficient C_F. A relationship between the yaw self-aligning torque spring constant k_{Mz} and the self-aligning torque coefficient C_M can also be derived. The resulting relations are

$$C_F = k_{F\phi}/(\lambda + h) \quad (22)$$

and

$$C_M = (k_{Mz}/h) \quad (23)$$

This small modification to string theory allows the use of two independent spring constants, $k_{F\phi}$ and k_{Mz}, in place of one spring constant, k_y. The usefulness of this modification will be discussed later.

Because the path frequency is the important parameter in string theory, the force and moment responses are found as a function of the dimensionless reduced frequency ($D\Omega/v_0$), where D is the tire diameter, Ω is the excitation frequency and v_0 is the road speed. The force and moment magnitudes can also be made dimensionless using the modeling laws discussed in Ref. 3.

Comparison of String Theory Predictions and Scale Model Measurements

For this study, small scale model tires of four different constructions were used to examine dynamic properties of tires. Two types were scaled versions of existing aircraft tires and were of conventional bias construction. One type was constructed without fabric reinforcement and was isotropic in its construction materials. The fourth type was an unbelted tire with one ply of radially-oriented fabric reinforcement, and as such represented a case of low tire lateral stiffness characteristics. The dimensions and properties of the different tires are given in Table I. During all subsequent tests reported here, the tires were operated under the conditions given in Table I. The tire properties shown are values obtained in tests described in Ref. 3.

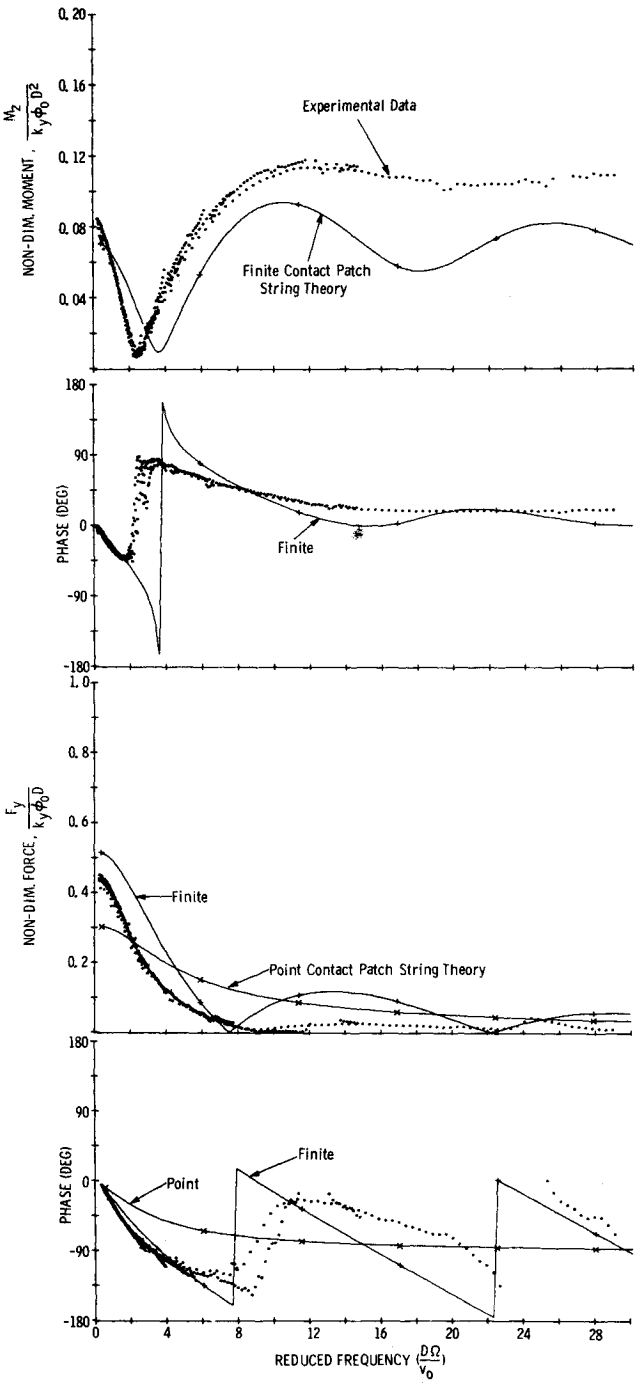

Fig. 6 Dimensionless force and moment response to steer excitation of tire A24.

The model tires described in Table I were run on The University of Michigan small scale roadwheel tire testing apparatus previously described in.[3] The tires were moved in either sinusoidal steer or sinusoidal lateral displacement by means of a harmonic displacement generator operating through a linkage system. The tires were run with excitation frequencies ranging from 0.1 to 10 H_z, amplitudes of 1.8–2.6° or 0.05–0.10 in., and at a range of surface velocities from 0.85 fps to 19.6 fps. Lateral force F_y and self-aligning torque M_z were recorded. The resulting data were analyzed using a swept frequency Fourier analysis program developed at the Bioelectrical Sciences Laboratory at The University of Michigan and described in Ref. 4. Tires were operated at several different roadwheel velocities but with continuously varying lateral or steer excitation frequency. This system allowed identification of resonant components associated with the natural frequencies

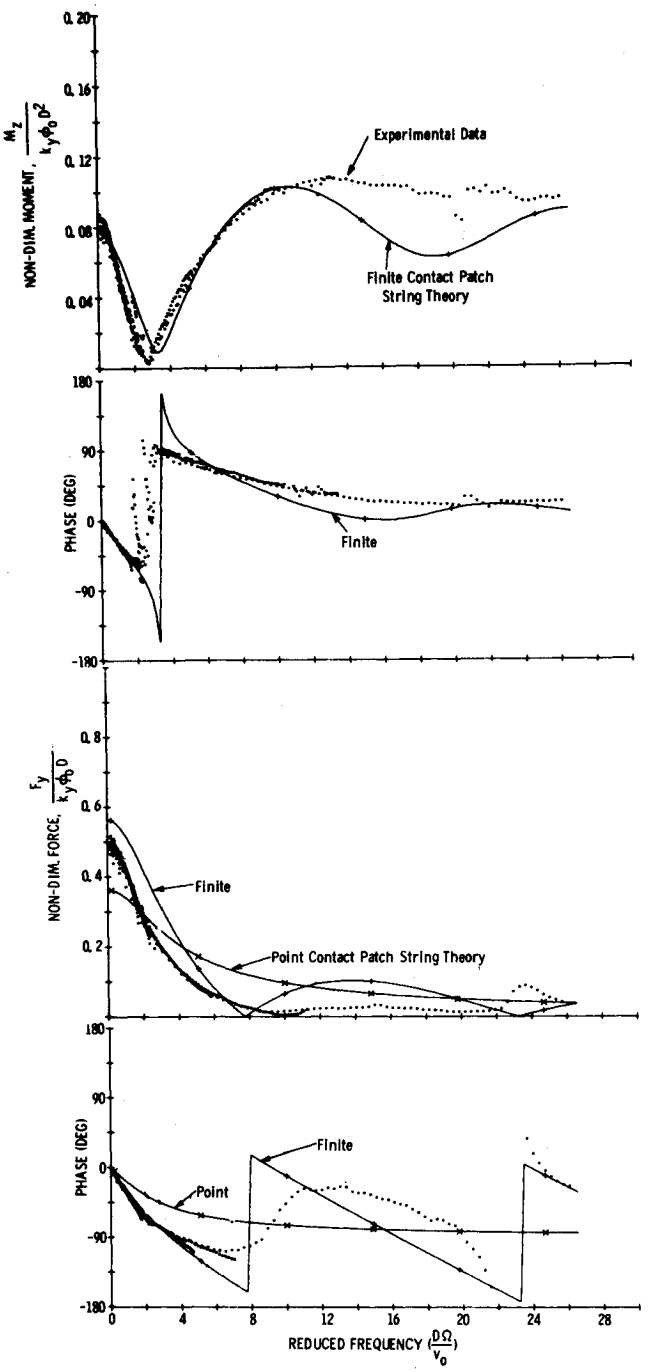

Fig. 7 Dimensionless force and moment response to steer excitation of tire B9.

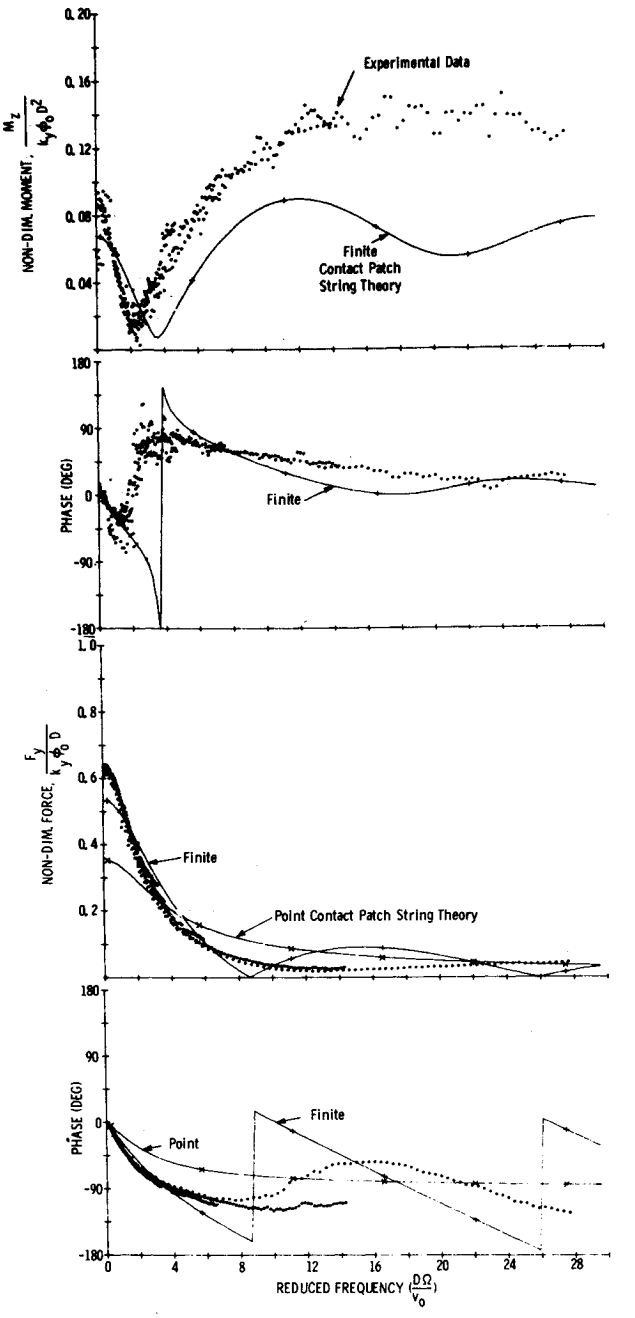

Fig. 8 Dimensionless force and moment response to steer excitation of tire VecoCL.

of mechanical portions of the roadwheel system. These resonant components could then be filtered out of tire response data.

Amplitude linearity was the first aspect of dynamic tire response to be studied. String theory predicts complete linearity of force and moment with respect to lateral displacement or steer angle. Figures 2 and 3 show the results for two different excitation amplitudes. The results indicate that the deviations from linearity are not major. The data presented in Fig. 2 for lateral excitation indicates self-aligning torque is relatively sensitive to amplitude. This result may be due to the sensitivity of self-aligning to slip in the contact patch and will be discussed further. The results shown in Fig. 3 for steer excitation show excellent linearity. The smaller steer amplitude is more susceptible to phase jump effects than the larger amplitude. The phase jump at 7.8 H_z was caused by system resonance and was not due to the tire. This result was discovered when the experimental results were reduced to the reduced frequency $\Omega D/v_0$. In reduced frequency form many of the test results overlap and the system resonance at 7.8 H_z becomes obvious.

The results in nondimensional form for lateral and steer excitation are shown in Figs. 4–9. For these results, the smaller excitation amplitude was used. The lateral excitation results shown in Figs. 4 and 5 indicate that string theory predictions are in fairly good agreement with experiment. The low experimental self-aligning torque amplitude shown in Fig. 5 may be due to friction and surface property conditions. While predicted amplitudes are high, 20% for force and 100% for moment, the phase angles are in good agreement with experiment.

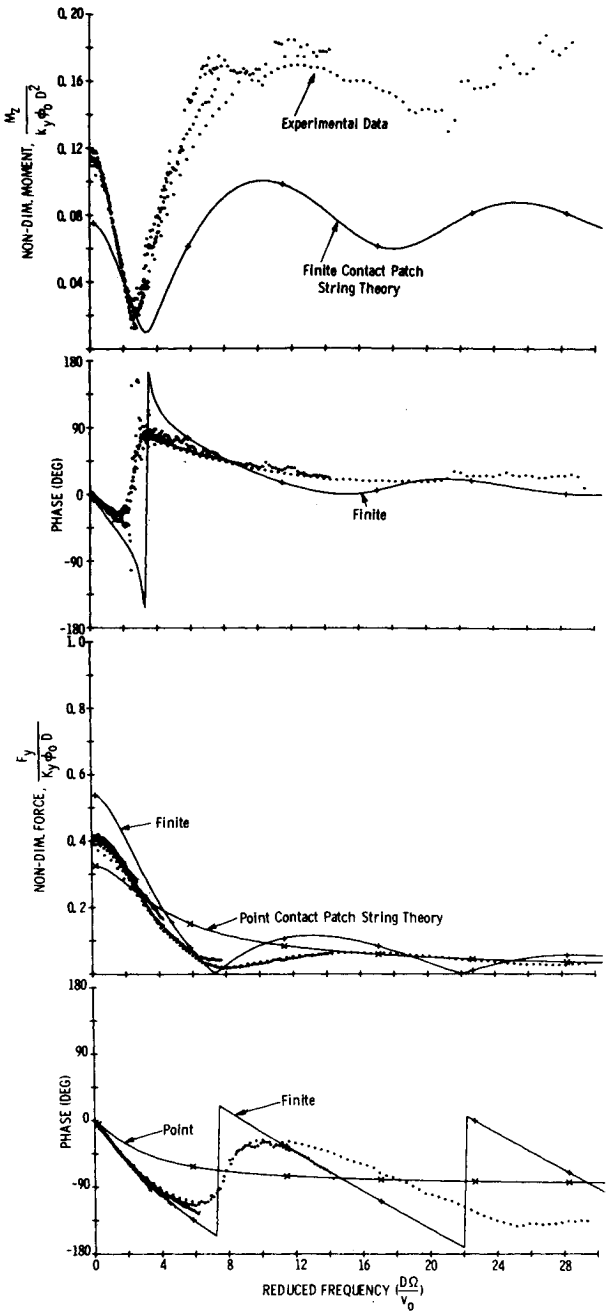

Fig. 9 Dimensionless force and moment response to steer excitation of tire RHCA12.

The steer excitation results shown in Figs. 6–9 indicate that this mode of excitation may be more fruitful for evaluation of theory than lateral excitation. The steer excitation results exhibit more characteristic features, especially the minimum moment and its phase jump. A brief analysis indicates that instability occurs to the left of this minimum and stability to the right. All four types of tires were tested in the steer excitation mode. The data points which were obvious system resonances were eliminated from the last four figures (while questionable points were retained).

The agreement between string theory predictions and experiment for the bias-type tires is good. However, the predicted results for the isotropic toroid and the unbelted tire are significantly lower than the experimental data. Better agreement is possible if the two constant modification to string theory discussed previously is used. The

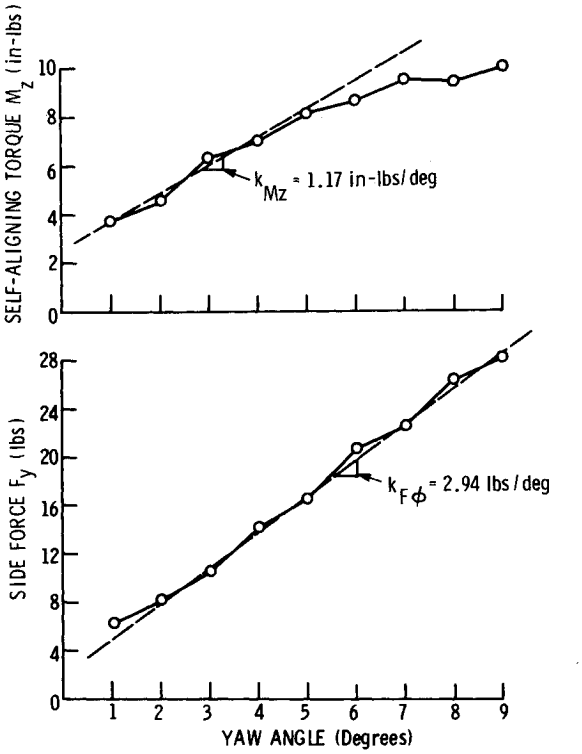

Fig. 10 Steady-state, yaw data at discrete yaw angles for tire A24.

modification requires the spring constants $k_{F\phi}$ and k_{Mz} taken at steady state yaw. The usual method for obtaining force and moment data is to run the tire at discrete yaw angles and plot the average amplitude versus yaw angle. Figure 10 shows typical data taken on tire A24 of this

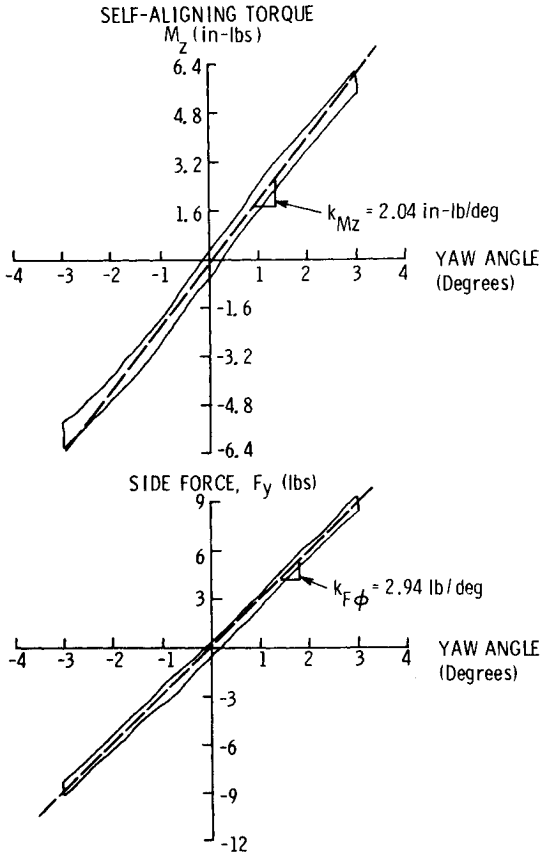

Fig. 11 Steady-state, continuous yaw data for tire A24.

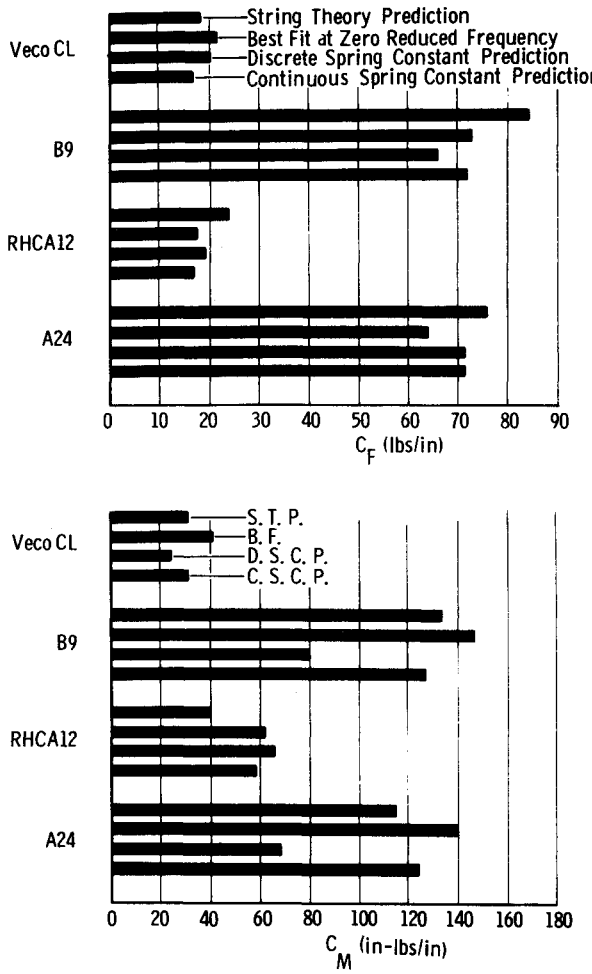

Fig. 12 Dynamic force and moment coefficients for four model tires.

study. An alternate method of obtaining such data is suggested by noting that the side force and moment response may be measured at low frequencies under dynamic steer conditions. Data taken under these conditions should approach steady state data. Figure 11 shows data measured using slow continuously varying yaw angles at a reduced frequency $D\Omega/v_0 = 0.009$. The force response from the data shown in Fig. 11 is quite linear for the entire range of swept angles and agrees well with steady-state data shown in Fig. 10. However, self-aligning torque response under continuously varying steer angles is linear only within a small range of yaw angles centered about zero. This result implies slip in the contact patch at relatively small steer angles. The resulting self-aligning torque stiffness k_{Mz} is much more accurate for dynamic work at small angles ($<3°$) than that derived from steady-state data.

Figure 12 shows a comparison of values of the dynamic force and moment coefficients, C_F and C_M, for the last four model tires whose dynamic properties are shown in Figs. 6–9. These coefficients are arrived at using four methods. In the first, the von Schlippe string theory predicts C_F and C_M coefficients by comparing Eq. (1) and (7) to Eqs. (19–20). Secondly, the best fit values of C_F and C_M are determined by using the two constant modification to string theory and by varying C_F and C_M until the theoretical predictions at zero reduced frequency agree with the experimental data at zero reduced frequency shown in Figs. 6–9. Finally, the discrete and continuous spring constant values are derived from Eqs. (22–23), using the two sets of slow-rolling experimental values of $k_{F\phi}$ and k_{Mz}.

The values of C_F are in relatively good agreement for all methods. However, the moment coefficient C_M is much more dependent upon the experimental method used to determine self-aligning torque. Subsequent comparison indicates, as noted previously, that the better method for determining C_M is to use data generated by slowly varying steer angle operation of the tire rather than steady-state steer conditions. This result again points up the extreme sensitivity of the self-aligning torque property of a tire. Self-aligning torque is apparently quite dependent upon local slip in the contact patch and on the nature of the friction surface. Basically, self-aligning torque is a small quantity whose origin lies in the difference between two forces, and hence might be expected to show sensitivity to such factors.

Conclusions

Comparisons between measured tire force and moment response, using small-scale models, and computations using the so-called string theory to describe the tire centerline displacement, show that in general string theory provides an adequate model for use in shimmy analyses of tire-wheel systems. While the calculated tire properties sometimes differ quantitatively from the measured properties, in all cases the trends are correct and in most cases quantitative agreement is surprisingly good. All such computations were performed using tire elastic properties obtained from static or slow rolling tests.

The two-constant modification of string theory allows an extra degree of freedom in matching predictions with observation. Slow rolling, continuously varying yaw angle data yields the added input parameters needed for the two-constant theory. For conventional bias-ply tires, the two-constant modification does not appear to be necessary. However, for other tire constructions the added flexibility may prove useful.

Based on these results, it seems quite probable that no significant improvement in the accuracy or validity of existing shimmy theories could be achieved by attempting to incorporate into them elastic properties of the tire gotten from high-speed or high-frequency dynamic tests. Not only are such tests extremely expensive, but based on these results such tests would not change shimmy predictions appreciably. Improvement in shimmy predictions must be sought in other areas.

References

[1]von Schlippe, B. and Dietrich, R., "Papers on Shimmy and Rolling Behavior of Landing Gears, presented at Stuttgart Conference, Oct. 16, 17, 1941," TN 1365, 1954, NACA.

[2]Moreland, W. J., "The Story of Shimmy," *Journal of the Aeronautical Sciences*, Vol. 21, No. 12, 1954, pp. 793–808.

[3]Clark, S. K., Dodge, R. N., Lackey, J. I. and Nybakken, G. H., "Structural Modeling of Aircraft Tires," *Journal of Aircraft*, Vol. 9, No. 2, Feb. 1972, pp. 162–167.

[4]Williams, W. J., Gesink, J. W., and Stern, M. M., "Biological System Transfer-Function Extraction Using Swept-Frequency and Correlation Techniques," *Medical and Biological Engineering*, Vol. 10, 1972, pp. 609–620.